OXIDATION OF A HAFNIUM DIBORIDE-BASED COMPOSITE

Martin C. Jischke

School of Aerospace, Mechanical and Nuclear Engineering, University of Oklahoma,
Norman, Oklahoma

A model of the high-temperature oxidation of a hafnium diboride-based composite is presented along with theoretical calculations of the response of a sample to an imposed constant heat flux.

A hafnium diboride-based composite, which we shall refer to as Gibsonite in honor of its inventor J. Gibson, has been experimentally observed to have superior oxidation resistance characteristics at high temperatures. For this reason, Gibsonite is being considered for re-entry protection of radioisotope heat sources. In order to gain a basic understanding of the Gibsonite oxidation process as well as to develop a capability for prediction of material behavior, the present study was conducted.

A MODEL FOR GIBSONSITE OXIDATION BEHAVIOR

Gibsonite is a high-temperature oxidation-resistant diboride composite, the composition of which, by weight percent, is given below.

Material	Weight %
HfB_2	66
SiC	15
Graphite (Thornel 50 fibers)	14
WSi_2	5

The composite is formed by hot pressing techniques with densities in excess of 90% of theoretical being obtained. In addition to the above composition, samples have been formed without WSi_2.

Detailed information on oxidation behavior of Gibsonite is not available. For this reason, it was necessary, in developing a physical model of Gibsonite oxidation, to rely heavily on experimental results obtained by others on similar, but different, materials. In particular, we have made extensive use of experimental results obtained, by Manlabs, Inc., Cambridge, Mass. (1-6), in an eight-year Air Force-sponsored study of the high-temperature oxidation resistance of diborides.

The understanding of Gibsonite behavior in a high-temperature oxidizing environment must be based upon a knowledge of the associated chemistry. To this end, consider exposing a sample of Gibsonite to a high-enthalpy-flux airflow in which the enthalpy level can be adjusted so as to yield various surface temperatures T_s.

For T_s less than 1700°K there is negligible oxidation of the composite for times of the order of tens of minutes. This is due, in part, to the formation of a very thin, glassy layer of SiO_2 which protects the composite from further oxidation, as well as to the low value of the oxygen diffusion coefficient at these temperatures.

At T_s equal to 1700°K there is evidence of formation of a thin surface layer of solid oxides (HfO_2, B_2O_3, SiO_2, W) with a small mass loss due to evolution of gaseous CO. The associated oxidation reactions are:

$$HfB_2 + 5/2\ O_2 \rightleftarrows HfO_2\ (s) + B_2O_3\ (s) \qquad \text{Eq. 1}$$

$$WSi_2 + 2\ O_2 \rightleftarrows W + 2\ SiO_2\ (s) \qquad \text{Eq. 2}$$

$$C + 1/2\ O_2 \rightleftarrows CO\ (g) \qquad \text{Eq. 3}$$

$$SiC + 3/2\ O_2 \rightleftarrows SiO_2\ (s) + CO\ (g) \qquad \text{Eq. 4}$$

The oxidation rates remain quite low (recession rates of the order of 10^{-6} cm/sec) with the solid B_2O_3 forming a protective layer. The interface between the solid oxide and virgin material has the qualities of an amorphous glass (Hf, B, Si, W; O_x) which enhances the adherence qualities of the oxide, especially in the presence of thermal stresses.

As the surface temperature increases from 1700°K to 1900°K, the B_2O_3 (s) sublimes to the gaseous phase affording protection

Proc. Okla. Acad. Sci. 53: 81-87 (1973)

to the underlying virgin material. At approximately 1900°K, the rate of evolving of B_2O_3 (g) equals the rate of formation of B_2O_3 (s) with the net effect of changing the oxidation reaction of HfB_2 to

$$HfB_2 + 2\,O_2 \rightleftarrows HfO\,(s) + B_2O_3\,(g) \qquad \text{Eq. 5}$$

As T_s increases beyond 1900°K, one begins to observe preferential oxidation of SiC, C, and WSi_2 according to

$$SiC + O_2 \rightleftarrows SiO\,(g) + CO\,(g) \qquad \text{Eq. 6}$$

$$C + 1/2\,O_2 \rightleftarrows CO\,(g) \qquad \text{Eq. 7}$$

$$WSi_2 + O_2 \rightleftarrows W + 2\,SiO\,(g) \qquad \text{Eq. 8}$$

leaving a (SiC, C, WSi_2)-depleted diboride zone between the surface oxide and the virgin Gibsonite as indicated below:

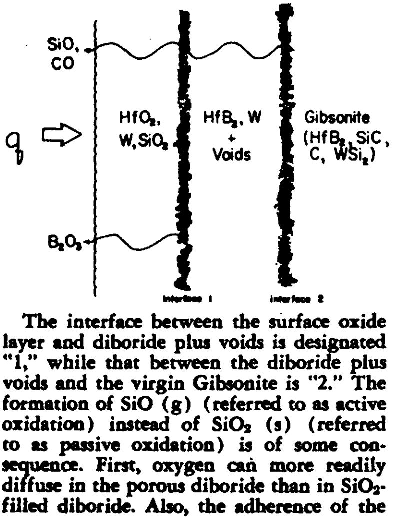

The interface between the surface oxide layer and diboride plus voids is designated "1," while that between the diboride plus voids and the virgin Gibsonite is "2." The formation of SiO (g) (referred to as active oxidation) instead of SiO_2 (s) (referred to as passive oxidation) is of some consequence. First, oxygen can more readily diffuse in the porous diboride than in SiO_2-filled diboride. Also, the adherence of the oxide to the virgin material is severely degraded owing to the absence of the glassy SiO_2. This passive to active oxidation transition will be discussed later to indicate an approximate calculation of the transistion temperature for various oxygen pressures. There is substantial evidence for the preferential oxidation of SiC and C in the Manlabs studies of HfB_2- and ZrB_2- based composites. Also, motion pictures of Gibsonite oxidation (7) show evidence of the evolution of CO gas.

Experimental data from Manlabs and Gulbranson, *et al* (8) suggest that the SiC recession rate to be linear in time with an Arrhenius temperature dependence and a $P_{O_2}^{0.8}$ pressure dependence. That is, under isothermal conditions

$$\frac{dX_2}{dt} = k_2(t) = A_2\, P_{O_2}^{0.8}\, e^{-T_{A_2}/T} \qquad \text{Eq. 9}$$

where the frequency factor A_2 and activation temperature T_{A_2} are independent of temperature. The HfB_2 recession rate is observed to be parabolic in time with an Arrhenius temperature dependence. Under isothermal conditions

$$\frac{dX_1}{dt} = k_1\,(t) = A_1\, e^{-T_{A_1}/T}\, t^{-1/2} \qquad \text{Eq. 10}$$

independent of the oxygen partial pressure. While this expression is not valid for very small times where the low-temperature data of Smeltzer and Simnad (9) for oxidation of hafnium show a logarithmic rate (700 - 1500°K), the initial kinetics are quite difficult to determine at higher temperatures. According to Wagner's diffusion theory for oxide scales with electronic conductivity predomination (10), the oxidation proceeds by means of inward diffusion of oxygen through anion vacancies and is, as observed, independent of the oxygen partial pressure.

The theoretical expression for the parabolic rate constant is (10)

$$k_1 = \frac{n}{2}\, C_o D_o^1 \left\{ \left(P_{O_2}^{1}\right)^{-1/n} - \left(P_{O_2}^{o}\right)^{-1/n} \right\} \qquad \text{Eq. 11}$$

where C_o is the oxygen vacancy concentration in the oxide and D_o^1 is the diffusion coefficient of oxygen atoms in the oxide, evaluated at the oxide-metal interface. The above is derived assuming that $D_o = D_o^1 P_{O_2}^{-1/n}$ is the dependence of the oxygen diffusion coefficient on oxygen pressure, appropriate to diffusion by oxygen vacancies in oxygen deficient or metal rich oxides ($D_{oxygen} >> D_{metal}$). Note that if the oxygen pressure at the oxide-metal interface, $P_{O_2}^{i}$, is negligible compared to the pressure at the air-oxide interface, $P_{O_2}^{1}$, $\left(P_{O_2}^{1}\right)^{-1/n} >> \left(P_{O_2}^{o}\right)^{-1/n}$, the rate constant is independent of the ambient oxygen pressure, as observed experimentally. It is important to note that the oxygen pressure at the metal-oxide interface is assumed to be equal to the equilibrium dissociation pressure of the oxide in contact with its metal. Assuming the Wagner theory to be correct, this result emphasizes the need for hot-pressing samples to densities as close to theoretical as possible. That is, as oxidation proceeds by means of vacancy diffusion, a smaller number of vacancies (*e.g.*, smaller C_0) implies a lower oxidation rate.

Our understanding of the underlying processes giving rise to the linear oxidation rate of SiC is much less certain. Kofstad (11) indicates that when porous scales are formed, the kinetics of the reaction are often linear in time. Such kinetics may result when a phase boundary process at the metal-oxide interface is rate-determining if the porosity of the oxide extends to the metal surface. Linear reaction rates often show an oxygen pressure dependence which indicates that oxygen adsorption is a rate-limiting factor in the overall process. In such cases the reaction mechanism is a complex one which comprises a two-or-more-part process, for example, adsorption and subsequent reaction.

The preceding description is valid as T_s increases to 2400°K. At 2400°K, the layer of SiO_2 at the air-oxide interface melts, leaving almost pure HfO_2 as sketched below.

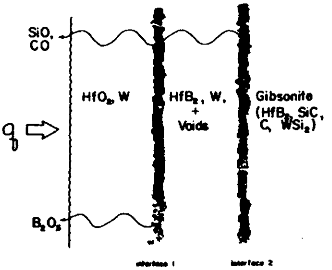

The HfO_2 scale is rather porous because of the gaseous CO, SiO, and B_2O_3 being evolved through it and is observed to be much less glassy than the SiO_2 surface. The pure HfO_2 is protective of the underlying material in part because of its rather low thermal conductivity.

Further increases in the surface temperature up to 3100°K simply lead to increased recession rates for interfaces 1 and 2. At 3100°K, the outer HfO_2 layer becomes molten and begins to flow under the action of aerodynamic pressure and shear forces. However, the HfO_2 retains its protective nature up to 3600°K. Also, at the front surface, HfO_2 begins to dissociate into HfO and oxygen.

At T_s equal to about 3600°K the underlying HfB_2 becomes molten and flows. The HfO_2 liquid surface layer is quite thin and flows readily, presumably because of the reduced viscosity of HfO_2 (1) at these temperatures. Under these conditions the material recession rates are substantial (in excess of 5×10^{-3} cm/sec) and the material no longer retains its structural integrity or protective nature.

The above discussion indicates that below 3100°K one would observe little or no recession of the air-oxide interface, although the SiC would be consumed by oxidation. That is, the fact that the material surface, as viewed, recedes a very small distance does not mean negligible material consumption. It simply means that the surface temperature is below the melting value. Also, in this regard, the mass change of a specimen upon oxidation results from two competing effects. First, there is the mass loss due to SiC, WSi_2, and C oxidation in which SiO and CO are given off. Second, there is a weight gain due to oxidation of the HfB_2 with B_2O_3 being given off. Thus, depending upon the relative values of the oxidation rates, one can have a mass gain or loss. Thus, there will be little correlation of mass loss with the air-oxide surface motion.

At noted earlier, the oxidation of SiC changes from a passive to an active form as the temperature increases or the pressure decreases. The important chemical reactions occurring in this phenomenon are listed below.

	Equilibrium Constants ($\log_{10} K$ [atm])			
	1400°K	1600°K	1800°K	
$SiC + \frac{3}{2} O_2 \rightleftarrows SiO_2\ (s) + CO$	30.60	26.26	22.89	Eq. 12
$SiC + O_2 \rightleftarrows SiO\ (g) + CO$	14.17	13.51	12.99	Eq. 13
$SiC + 2\ SiO_2 \rightleftarrows 3\ SiO(g) + CO$	-18.90	-11.98	- 5.58	Eq. 14

The reaction of passive oxidation (Eq. 12) occurs at low temperatures and high oxygen pressures, while active oxidation (Eq. 13) occurs at high temperatures and low oxygen pressures. The rate of Eq. 12 is al-

TABLE 1. *Input data for numerical computations*[a]

	Case 1	Case 2	Case 3	Case 4
q_{applied} (ergs/cm^{2}sec)	1.57×10^9	5.79×10^8	2.84×10^9	3.38×10^9
(BTU/ft^{3}sec)	138	51	250	300
h (cal/gm)	1.52×10^4	9.62×10^2	5.57×10^3	1.8×10^4
P_{O_2} (atm)	3.02×10^{-2}	1.04×10^{-3}	4.0×10^{-2}	2.0×10^{-2}
P (atm)	1.51×10^{-1}	5.2×10^2	2.0×10^{-1}	1.0×10^{-1}
$t_{\text{reference}}$ (sec)	1.35×10^3	6.04×10^2	5.56×10^2	4.28×10^2

[a] In all cases, the following parameter values were used.

$k = 0.3$ cal/sec cm$^{\circ}$K
$\rho\Delta H_{32} = -8.20 \times 10^3$ cal/cm^3
$\rho_2\Delta H_{21} = -1.3 \times 10^4$ cal/cm^3
$\eta = 0.8$
$T_i = 300\ ^{\circ}$K
$A_1 = 7.90 \times 10^{-2}$ cm/ sec$^{1/2}$
$A_2 = 3.80 \times 10^{-2}$ cm/sec
$T_{A_2} = 8.2 \times 10^3\ ^{\circ}$K
$T_{A_1} = 1.4 \times 10^4\ ^{\circ}$K
$\epsilon = 0.75$
$W_{si} = 0.11$
$W_o = 0.19$
$W_B = 0.07$
$W_{Hf} = 0.59$
$W_W = 0.04$

most independent of oxygen pressure while Eq. 13 shows a $P_{O_2}^{\ 0.8}$ dependence. Wagner (12) has shown that Eq. 12 occurs for P_{O_2} above a critical maximum, P_{O_2} (max.), while Eq. 13 occurs for P_{O_2} below this value. Wagner derives a theoretical expression for P_{O_2} (max.) which can be reduced to

$$P_{O_2}\ (\text{max.}) \approx 1.13 \times 10^9 \exp\left(-\frac{4.53 \times 10^4}{T}\right) \quad \text{Eq. 15}$$

assuming that Eq. 14 is the transition reaction. This result is sketched in Figure 1. As indicated, active oxidation is most likely above 2200°K.

In closing this discussion, it is emphasized that the physical model described, while based upon and agreeing generally with available experimental information, may require corrections as more data is taken. There is uncertainty in the various temperatures at which different processes occur. Also, most of the description has been derived from observation of behavior of HfB_2-SiC-C composites which do not contain WSi_2 and have much higher diboride and lower graphite contents. The effect of forty-three volume percent graphite on the various reaction mechanisms is not well understood.

THEORETICAL CALCULATIONS

Consider a slab of Gibsonite which at some initial instant $t = 0$ is subjected to a heat flux q_{applied}. For simplicity the discussion is limited to the situation where melting of the HfO_2 does not occur. Hence, the model should be valid for surface temperatures below approximately 3100°K. Also, a one-dimensional semi-infinite slab geometry is considered. A sketch illustrating the nomenclature is given below.

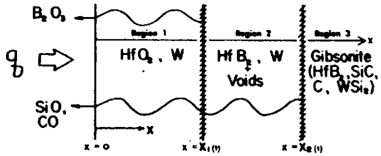

Estimation of typical reaction and heating rates shows that the sample heats up rather quickly in comparison with the rate at which the two interfaces recede. That is, if we define   as the thermal layer thickness, then $\delta >> X_1, X_2$. The temperature at the two interfaces will then be quite close to the surface temperature. Thus, to a first approximation in the determination of the transient temperature in the sample, we can neglect regions 1 and 2 except as they affect the energy balance near the surface X = 0. That is, we include the energy evolved in the oxidation at interfaces 1 and 2 in an effective heterogeneous combustion term in the energy balance at X = 0. We refer to this as the "surface reaction approximation" in which the region from X = 0 to X = X_2 is considered to be an infinitesimally thin reaction zone.

Conservation of energy within the slab then reflects a balance between energy conducted through the solid and energy stored internally. Thus can be written

$$\rho c \frac{\partial T}{\partial t} = \frac{\partial}{\partial X}\left(k \frac{\partial T}{\partial X}\right) \qquad 0 < X < \infty \qquad \text{Eq. 16}$$

where ρ is density, c is specific heat, K is thermal conductivity, and T is temperature. The boundary condition at X = 0 reflects conservation of energy

$$X = 0: \quad -k \frac{\partial T}{\partial X} = q_{applied} - \epsilon\sigma T^4 - \dot{m}_g \eta (h_\infty - h_s) \qquad \text{Eq. 17}$$

$$+ \rho\Delta H_{32} \frac{dX_2}{dt} + \rho_2 \Delta H_{21} \frac{dX_1}{dt} \quad . \qquad \text{Eq. 18}$$

Here $\epsilon \sigma T^4$ is the reradiated energy flux to the assumed low temperature environment with ϵ the surface emissivity and α the Stefan-Boltzmann constant. $\dot{m}_g \eta (h_\infty - h_s)$ is the aerodynamic blockage heat flux where m is the mass flux of gas evolved at the surface,   is an empirical blockage factor, and $(h_\infty - h_s)$ is the enthalpy difference between the boundary layer edge and X = 0. $\rho \Delta H_{32}\, dx_2/dt$ is the energy flux absorbed in the reaction at interface 2 where ΔH_{32} is the enthalpy per unit mass of reactants (positive for endothermic reactions) and dx_2/dt is the rate of recession of interface 2. Similarly $\rho_2 \Delta H_{21}\, dx_1/dt$ is the energy flux absorbed at interface 2 where ρ_2 is the density of the material in region 2. Heterogeneous combustion and sublimation have been neglected as experiment suggests these effects to be unimportant. Also, the temperature far away from the surface must return to some given value.

$$X \longrightarrow \infty: \quad T \longrightarrow T_1 \qquad \text{Eq. (19)}$$

and the initial configuration is to be unoxidized.

$$t = 0: \quad X_1(0) = X_2(0) = 0, \; T(X,0) = T_1 \qquad \text{Eq. (20)}$$

This formulation is still incomplete. It is necessary to specify how the various interface positions are to be determined. Such a determination from first principles depends upon a knowledge of the combined effects of heterogeneous chemical reactions, diffusion, and unsteady conduction. Assuming Wagner's theory of parabolic oxidation (10) is valid, interface one is located by the condition that the partial pressure of oxygen at the metal-oxide interface is equal to the equilibrium dissociation pressure of the oxide in contact with its metal. Thus, one must determine the oxygen pressure as a function of time and position, taking account of the strong temperature dependence of the diffusion coefficient, the temperature being a function of position and time as a result of the unsteady nature of the conduction process. There are not sufficient data at this time to support such a calculation.

The conditions locating interface 2 are much less obvious. Although the data of Gulbranson, et al (8) show a pressure dependence suggesting a diffusion-limited process, it is not apparent how this would lead to the observed constant recession rate in time. Kofstad's (11) suggestion of a two-or-more-part process is reasonable although no actual mechanism can be offered at this time.

The approach here is empirical. That is, we propose to correlate data on recession rates obtained from experiments on similar diboride composites. With regard to the HfB_2 oxidation, experiments on a wide range of composites indicate a parabolic oxidation rate. An even larger body of data on SiC oxidation shows a linear oxidation rate. One subtlety should be mentioned. All experimental data has been obtained for isothermal samples. A question then arises as to the proper application of these results to nonisothermal samples. With regard to the SiC oxidation, we assume that the recession rate at any time t depends upon the temperature at interface 2.

$$\frac{dX_2}{dt} = A_2 \, P_{O_2}^{0.8} \exp\left(-\frac{T_{A_2}}{T(X_2(t),t)}\right) \quad \text{Eq. 21}$$

For the HfB_2 oxidation, we assume superposition to be valid. That is, as the movement of interface one is diffusion controlled, the linearity of Fick's law suggests such a superposition (assuming the appropriate diffusion coefficient is independent of concentration). Thus

$$\frac{dX_1}{dt} = k_1(0)t^{-1/2} + \int_0^t \frac{dk_1}{dt'}(t')\,(t-t')^{-1/2}\,dt' \quad \text{Eq. 22}$$

where

$$k_1(t) = A_1 \exp\left[-\left(\frac{T_{A_1}}{T(X_1(t),t)}\right)\right] \quad \text{Eq. 23}$$

This result, of course, agrees with the isothermal value.

To complete the description, we must evaluate the various gaseous mass-flow-rate terms. Neglecting the storage of gas in the pores of the oxide, the mass flow rate of each gas in the different regions must be constant, given by the rate at which the gas is evolved or consumed at the bounding interface. Thus, we can write

$$\dot{m}_g = \rho\left(W_{si}\frac{M_{sio}}{M_{si}} + W_c\frac{M_{co}}{M_c} - W_{si}\frac{M_o}{M_{si}} - W_c\frac{M_o}{M_c}\right)\frac{dX_2}{dt}$$
$$+ \rho_2\left(W_B\frac{M_{B_2O_3}}{M_{B_2}} + W_{Hf}\frac{M_{O_2}}{M_{Hf}} - W_B\frac{3M_o}{M_{B_2}}\right)\frac{dX_1}{dt} \quad \text{Eq. 24}$$

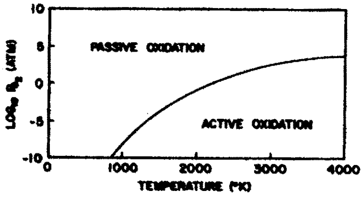

FIGURE 1. SiC passive to active oxidation boundary.

where the W's refer to the mass fractions of the various constituents in the virgin material and the M's refer to the molecular weights of the species. This completes the mathematical formulation of the problem.

The nonlinearity of the governing equations and boundary conditions make analytical solutions to the problem unlikely. Also, "exact" numerical solutions to this problem by, for example, finite difference methods are rather time-consuming both in programming effort as well as in computation. With this in mind, solutions to the surface reaction approximation have been attempted by means of the heat-balance integral method of Goodman (13). The method, analogous to the Karman-Pohlhausen technique of boundary layer theory, reduces the partial-differential heat conduction equation to an ordinary differential equation which can be solved readily by numerical means. As the method is well documented in standard texts (see, *e.g.*, reference 14), we shall not discuss the details but shall merely indicate some typical results. Table 1 lists the four sets of conditions typical of those envisoned in applications, for which results were obtained. The results are shown in Figures 2-3 where the surface temperature and the mass loss are given as functions of a normalized time (the normalization is given in Table 1). The results shown in Figure 3 indicate that, for the conditions considered, the mass loss is quite small. For example, the result for case 4 yields a mass loss of 0.028 grams/cm² after 428 sec. While the lack of

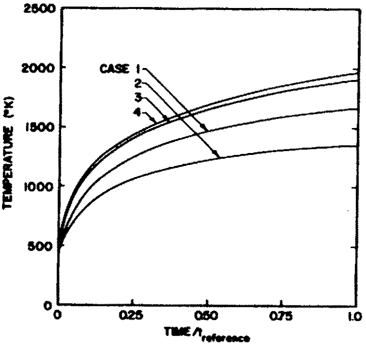

FIGURE 2. Variation to surface temperature with time.

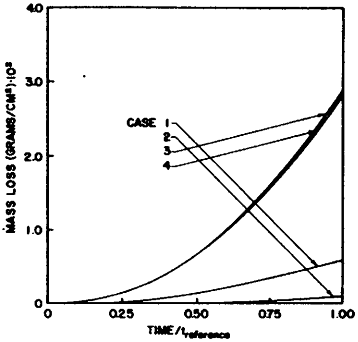

FIGURE 3. Mass loss variation with time.

data prevents a direct comparison with experiment, this low value is consistent with observation.

ACKNOWLEDGMENT

This work was conducted under the NORCUS Program sponsored by the Atomic Energy Commission.

REFERENCES

1. L. KAUFMAN and E. V. CLOUGHERTY, *Investigation of Boride Compounds for Very High Temperature Applications*, Part I, AFML RTD-TDR-63-4096, Air Force Materials Laboratory, Wright Patterson Air Force Base, Ohio, 1963.
2. L. KAUFMAN and E. V. CLOUGHERTY, *Investigation of Boride Compounds for Very High Temperature Applications*, Part II, AFML-RTD-TDR-63-4096, Air Force Materials Laboratory, Wright Patterson Air Force Base, Ohio, 1965.
3. L. KAUFMAN and E. V. CLOUGHERTY, *Investigation of Boride Compounds for Very High Temperature Applications*, Part III, AFML-RTD-TRD-63-4096, Air Force Materials Laboratory, Wright Patterson Air Force Base, Ohio, 1966.
4. E. V. CLOUGHERTY, D. KALISH, and E. T. PETERS, *Research and Development of Refractory Oxidation-Resistant Diborides*, AFML-TR-68-190, Air Force Materials Laboratory, Wright Patterson Air Force Base, Ohio, 1968.
5. E. V. CLOUGHERTY, K. E. WILES, and R. P. TYE, *Research and Development of Refractory Oxidation-Resistant Diborides*, Part II, Vol. V, *Thermal, Physical, Electrical, and Optical Properties*, AFML TR-68-190, Air Force Materials Laboratory, Wright Patterson Air Force Base, Ohio, 1969.
6. E. V. CLOUGHERTY, *Research and Development of Oxidation-Resistant Diborides*, Part II, Vol. I, *Summary*, AFML TR-68-190, Air Force Materials Laboratory, Wright Patterson Air Force Base, Ohio, 1970.
7. *Plasma Arc Ablation Tests for ATJ Graphite and Gibsonite*, Aerojet General Space Division Report 8018-F1, Aerojet General Corporation, Los Angeles, Calif., 1971.
8. E. A. GULBRANSEN, K. F. ANDREW, and F. A. BRASSART, J. Electrochem. Soc. 113: 1311-1314 (1966).
9. W. W. SMELTZER and M. T. SIMNAD, Acta Metall. 5: 328-334 (1957).
10. C. WAGNER, Zeit. Physik. Chem. 21: 25-29 (1933).
11. P. KOFSTAD, *High Temperature Oxidation of Metals*, J. Wiley and Sons, New York, 1966.
12. C. WAGNER, J. Appl. Physics 29: 1295-1297 (1958).
13. T. R. GOODMAN, ASME Trans. 80: 335-342 (1958)
14. M. N. OZISIK, *Boundary Value Problems of Heat Conduction*, International Textbook Co., Scranton, Pa., 1968.